International Journal of Concrete Structures and Materials
Vol.5, No.1, pp.35~42, June 2011
DOI 10.4334/IJCSM.2011.5.1.035

Design Equation for Punching Shear Capacity of SFRC Slabs

Hiroshi Higashiyama,[1)] Akari Ota,[2)] and Mutsumi Mizukoshi[3)]

(Received December 8, 2010, Revised January 24, 2011, Accepted January 28, 2011)

Abstract: In this paper, a design equation for the punching shear capacity of steel fiber reinforced concrete (SFRC) slabs is proposed based on the Japan Society of Civil Engineers (JSCE) standard specifications. Addition of steel fibers into concrete improves mechanical behavior, ductility, and fatigue strength of concrete. Previous studies have demonstrated the effectiveness of fiber reinforcement in improving the shear behavior of reinforced concrete slabs. In this study, twelve SFRC slabs using hooked-ends type steel fibers are tested with varying fiber dosage, slab thickness, steel reinforcement ratio, and compressive strength. Furthermore, test data conducted by earlier researchers are involved to verify the proposed design equation. The proposed design equation addresses the fiber pull-out strength and the critical shear perimeter changed by the fiber factor. Consequently, it is confirmed that the proposed design equation can predict the punching shear capacity of SFRC slabs with an applicable accuracy.

Keywords: steel fiber reinforced concrete, reinforced concrete slabs, punching shear capacity, cracks, fiber pull-out strength, fiber factor.

1. Introduction

Fiber reinforced concrete (FRC) has been used successfully in structures subjected to bending and/or shear. Punching shear failure in slabs occurs suddenly with little or no warning before collapse. FRC can improve such an undesirable failure and increase the strength of slabs with ductility at the point of failure. Previous studies have demonstrated the effectiveness of fiber reinforcement in improving the shear behavior of reinforced concrete slabs.[1-12] According to their investigations, fibers not only delay the formation of diagonal cracking within the slab and enable extensive cracking to occur at failure compared with slabs without fiber reinforcement, but also transform brittle-type punching shear failure into a gradual and ductile shear failure. Narayanan and Darwish[3] and Theodorakopoulos and Swamy[10,11] have proposed the predicting equation for the punching shear capacity of steel fiber reinforced slab-column connections. Narayanan and Darwish[3] considered the split cylinder strength of fiber reinforced concrete with its compressive strength, fiber factor,[13] and fiber pull-out stress[14] in the predicting equation. Moreover, they observed that the distance from the circumference of the column stub to the intersection of the shear crack and the plane of tension steel reinforcement decreased, as the fiber factor given by Narayanan and Kareem-Palanjian[13] became greater. The fiber factor is a combined parameter with fiber length and diameter, a fiber volume fraction, and a bond factor. Tan and Paramasivam[5] mentioned that the predicting equation[3] generally overestimates the punching shear capacity of SFRC slabs tested in their study. Theodorakopoulos and Swamy[10,11] have proposed the design equation based on their theoretical analysis. They considered the neutral axis depth accounting for the steel strain hardening effect and the fiber pull-out strength.

The objectives of this paper were to investigate the punching shear behavior of SFRC slabs and to propose the design equation based on the JSCE equation for reinforced concrete slabs.[15] In this study, 12 SFRC slabs were tested with varying amounts of steel fiber, slab thickness, tension steel reinforcement ratio, and compressive strength to obtain test data. Furthermore, test data of 50 SFRC slabs conducted by earlier researchers[1-3,6,9,12] were involved to verify the proposed design equation.

2. Review of previous equations

The Japan Society of Civil Engineers (JSCE) equation[15] for predicting the punching shear capacity of reinforced concrete slabs is given as follows:

$$V_u = \beta_d \beta_p \beta_r f_{pcd} u_p d \tag{1}$$

$$f_{pcd} = 0.2\sqrt{f_c'} \tag{2}$$

$$\beta_d = \sqrt[4]{\frac{1000}{d}} \tag{3}$$

$$\beta_p = \sqrt[3]{100\rho} \tag{4}$$

$$\beta_r = 1 + \frac{1}{1 + 0.25u/d} \tag{5}$$

$$u_p = u + \pi d \tag{6}$$

[1)]Dept. of Civil and Environmental Engineering, Kinki University, Higashiosaka, Osaka, 577-8502, Japan.
Email: h-hirosi@civileng.kindai.ac.jp.
[2)]Graduate School of Science and Engineering Research, Kinki University, Higashiosaka, Osaka, 577-8502, Japan.
[3)]Dept. of Civil Engineering, Kagawa National College of Technology, Takamatsu, Kagawa, 761-8058, Japan.

where f'_c is the cylindrical compressive strength of concrete (N/mm^2), d is the average effective depth (mm), ρ is the average tension steel reinforcement ratio, u is the perimeter of the loading pad (mm), and u_p is the perimeter of the critical section located at a distance of $d/2$ from the edge of the loading pad (mm). The values of f_{pcd}, β_d, and β_p are limited to 1.2 N/mm^2, 1.5, and 1.5.

Narayanan and Darwish[3] have provided the design equation for the punching shear capacity of SFRC slabs considering three factors: the strength of the very narrow compressive zone above the top of the inclined cracks; the pull-out forces on the fibers along inclined cracks; and the shear force carried by dowel and membrane actions which contribute the shear capacity. The design equation for the ultimate punching shear capacity of SFRC slabs is as follows:

$$V_{uf} = \xi_S(0.24f_{spf} + 16\rho + 0.41\tau F)b_{pf}\,d \tag{7}$$

$$f_{spf} = \frac{f_{cuf}}{20 - \sqrt{F}} + 0.7 + \sqrt{F} \tag{8}$$

$$b_{pf} = (4r + 3\pi h)(1 - KF) \tag{9}$$

$$F = \frac{L}{D}V_f d_f \tag{10}$$

$$\xi_s = 1.6 - 0.002h$$

where f_{cuf} is the cubic compressive strength of fiber reinforced concrete, f_{spf} is the computed value of split cylinder strength of fiber reinforced concrete, ρ is the tension steel reinforcement ratio, V_f is the fiber volume fraction, τ is the average fiber-matrix interfacial bond stress taken as 4.15 N/mm^2, d_f is the bond factor, h is the slab thickness, d is the effective depth, b_f is the perimeter of the critical section, K is the non-dimensional constant value (= 0.55), L and D are the length and the diameter of fiber, respectively, F is the fiber factor, and ξ_s is the empirical depth factor.

Theodorakopoulos and Swamy[10] have proposed the simple analytical model to predict the punching shear capacity of slab-column connections without and with fibers. Furthermore, they have presented a design equation modified the analytical model in order to avoid the repetitive process in the calculation of the neutral axis depth. Their design equation[11] for the ultimate punching shear capacity of SFRC slab-column connections is as follows:

$$V_{u\mathrm{F}} = m\left[0.234f_{cu}^{2/3}(4r + 12d)\frac{\alpha\lambda + \beta}{1 + \alpha\lambda + 1.25\beta}d(100/d)^{1/6}\right] + 2\sigma_{cu}\left[r + 0.866\frac{\alpha\lambda + \beta}{1 + \alpha\lambda + 1.25\beta}d\right]\frac{\alpha\lambda + \beta}{1 + \alpha\lambda + 1.25\beta}d \tag{12}$$

$$\sigma_{cu} = \eta_o\eta_b\left(\frac{l_f}{d_f}\right)V_f(m\,\tau) \tag{13}$$

$$\alpha = \frac{\rho f_y}{0.145f_{cu}} \tag{14}$$

$$\beta = \frac{\sigma_{cu}}{0.145f_{cu}} \tag{15}$$

where m is the coefficient depending on the concrete type, f_{cu} is the cubic compressive strength, r is the column side length, d is the effective depth, σ_{cu} is the ultimate tensile strength of fiber concrete, η_o is the 3-D fiber orientation factor, η_b is the bond factor, l_f and d_f are the length and the diameter of fiber, respectively, V_f is the fiber volume fraction, τ is the fiber-concrete interfacial shear stress taken as 4.15 N/mm^2, ρ is the tension steel reinforcement ratio, f_y is the yield steel strength, λ is the coefficient being available from the represented equations in the literature.[11]

3. Experimental program

3.1 Materials

For concrete, normal-weight ready mixed concrete delivered by an agitator truck from a local batch plant was used. Mixture proportions of the concretes are given in Table 1. For cement, normal Portland cement was used. The plain concretes were designed with a slump of 150 mm. Fine and coarse aggregates were blended with two kinds of aggregate, respectively. The maximum size of coarse aggregates was 20 mm. For admixture, an air entraining and water reducing agent was used. Hooked-ends type of steel fiber used was a 30 mm long with a diameter of 0.62 mm as shown in Fig. 1. According to the manufacturer, the 0.2 % offset yield strength, ultimate strength, and modulus of elasticity were 1119 N/mm^2, 1215 N/mm^2, and 184 kN/mm^2. In this study, SFRCs with six fiber volume fractions were prepared. Steel fibers were

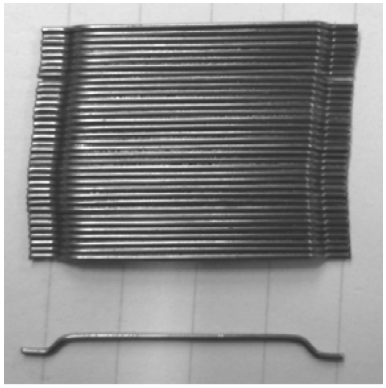

Fig. 1 Hooked-ends type steel fiber.

Table 1 Mixture proportions of plain concretes.

Mix no.	Unit weight (kg/m^3)					
	Water	Cement	Fine aggregates		Coarse aggregates	
			Mixed sand	Crushed sand	Crushed gravel	Lime stone
1	183	321	477	317	696	301
2	183	345	466	310	696	301

Table 2 Compressive strength and modulus of elasticity.

Mix no.	Fiber volume fraction (%)	Compressive strength (N/mm^2)	Modulus of elasticity (kN/mm^2)
1	0.63	27.8	19.2
1	0.67	24.6	22.6
2	0.72	42.4	29.6
2	0.91	21.6	21.4
1	0.94	31.1	24.0
1	1.03	30.4	24.0

thrown into the agitator drum at the laboratory. After that, the agitator drum was rotated at high speed for five minutes. After casting, the content of steel fibers in SFRC was immediately evaluated by water screening method using three prisms of 100 × 100 × 400 mm referred to JSCE-F 554-1999.[16] As the results, the effective fiber volume fraction for each mixture was 0.63%, 0.67%, 0.72%, 0.91%, 0.94% or 1.03 %. Standard deviation for the fiber volume fractions was within the range of 0.021 to 0.055. For each mixture, three cylinders of ϕ100 × 200 mm were cast for compressive strength and modulus of elasticity determination as per JSCE-G 551-1999.[16] Compressive strength and modulus of elasticity at the testing age are given in Table 2. Since compressive strength specimens were cured under uncontrolled laboratory environment together with corresponding SFRC slabs, the compressive strength and modulus of elasticity had influence of the casting season and the curing condition.

3.2 SFRC slabs

SFRC slabs were cast and compacted by a needle vibrator and cured under uncontrolled laboratory environment until the ready for testing. Table 3 gives the details of SFRC slabs tested in this study. The SFRC slabs, which were varied in slab thickness, steel fiber dosage, tension steel reinforcement ratio, and compressive strength, were 1200 mm square as shown in Fig. 2 (for example: t100-0.67). Reinforcing bars with a deformed shape, 9.53 mm (D10, SD295A) in a diameter and yield strength of 377 N/mm^2 were arranged in only tension layer. For all SFRC slabs, an arrangement spacing of reinforcing bars was uniform at 120 mm.

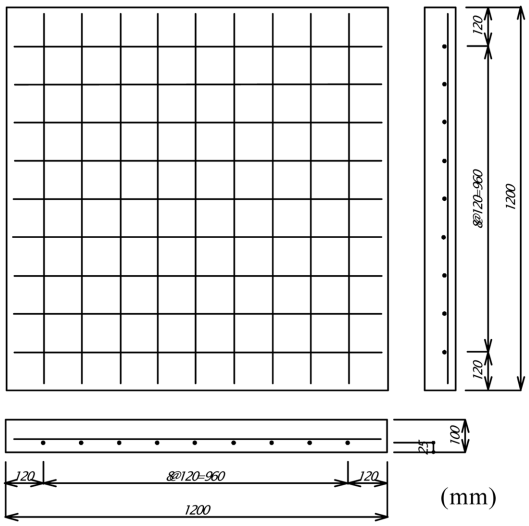

Fig. 2 Specimen size and reinforcement arrangement (t100-0.67)..

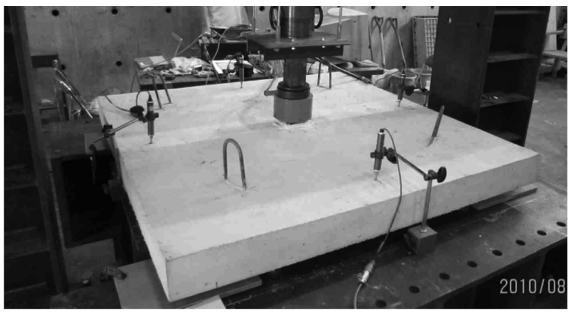

Fig. 3 View of test setup.

3.3 Test setup

Figure 3 shows the view of the test setup. All SFRC slabs tested were simply supported along four edges with a span length of 1000 mm. Slab corners were free to uplift during the loading test. Since the span length was relatively short, no influence of the uplift at the slab corners on the punching shear capacity was con-

Table 3 Details of SFRC slabs tested.

Slabs	Thickness (mm)	Effective depth (mm)	Reinforcement ratio (%)	Fiber volume fraction (%)	Length of loading pad (mm)	Maximum load (kN)
t100-0.67	100	70	0.85	0.67	100	137.5
t140-0.67	140	110	0.54	0.67	100	210.2
t180-0.67	180	150	0.40	0.67	100	297.6
t100-0.72	100	65	0.91	0.72	100	140.8
t140-0.72	140	105	0.57	0.72	100	213.2
t180-0.72	180	145	0.41	0.72	100	290.7
t100-0.91	100	65	0.91	0.91	100	120.8
t140-0.91	140	105	0.57	0.91	100	183.1
t180-0.91	180	145	0.41	0.91	100	231.2
t100-0.63	100	70	0.85	0.63	100	152.3
t100-0.94	100	70	0.85	0.94	100	147.9
t100-1.03	100	70	0.85	1.03	100	158.9

sidered. Concentrated load was applied at the center of the slab by a hydraulic jack through a square steel plate of 100 × 100 mm. The vertical displacement at the center of the slab and the settlement on the supported lines were monitored by linear variable displacement transducers (LVDTs) as shown in Fig. 3. In addition, cracking patterns on the bottom surface of all slabs were recorded and only two slabs with a thickness of 180 mm were sawn by a concrete cutter after testing to observe the punching shear cracks in the slabs.

4. Results and discussions

4.1 Punching shear behaviors

Failure mode of all SFRC slabs tested was punching shear. Relationships between applied load and deflection at the center of the slab are shown in Fig. 4. All SFRC slabs showed a gradual and ductile behavior beyond the maximum load in comparison with reinforced concrete slabs without fiber content. From Figs. 4(a) to (c), the punching shear capacity increased with a corresponding increase in the slab thickness. For each fiber volume fraction, the punching shear capacities of SFRC slabs with a thickness of 140 mm and 180 mm increased at 1.5 times and 2.0 times in comparison with that of SFRC slab with a thickness of 100 mm, respectively as given in Table 3. The deflection behaviors of the descending part beyond the maximum load were different with the slab thickness. The residual resistance to load considerably decreased with increasing the slab thickness.

In contrast, the punching shear behaviors of SFRC slabs with a thickness of 100 mm were almost identical close to the maximum load as shown in Fig. 4(d), though the fiber volume fraction was varied. The maximum loads including other SFRC slabs with a thickness of 100 mm did not linearly increase with increasing the fiber volume fraction. This trend is the same as the results presented by Mindess, et al.[17] They showed that the increase of the

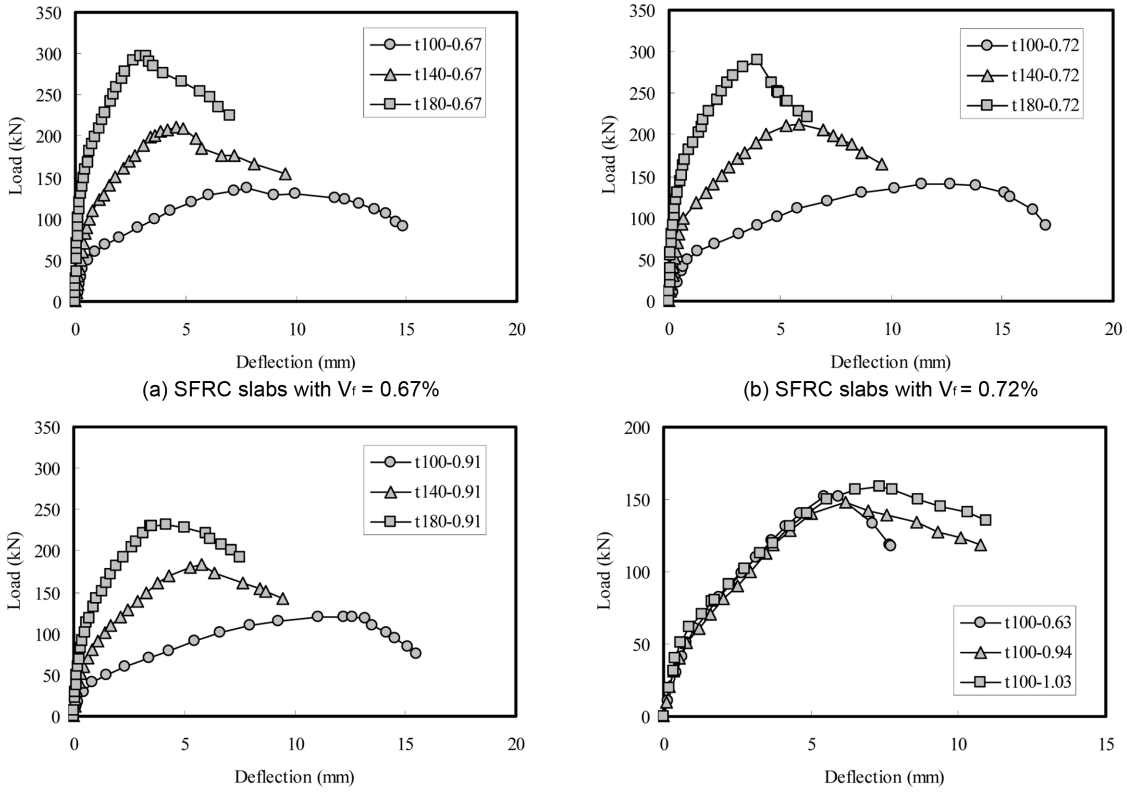

(a) SFRC slabs with V_f = 0.67%
(b) SFRC slabs with V_f = 0.72%
(c) SFRC slabs with V_f = 0.91%
(d) SFRC slabs with various V_f

Fig. 4 Applied load and deflection curves.

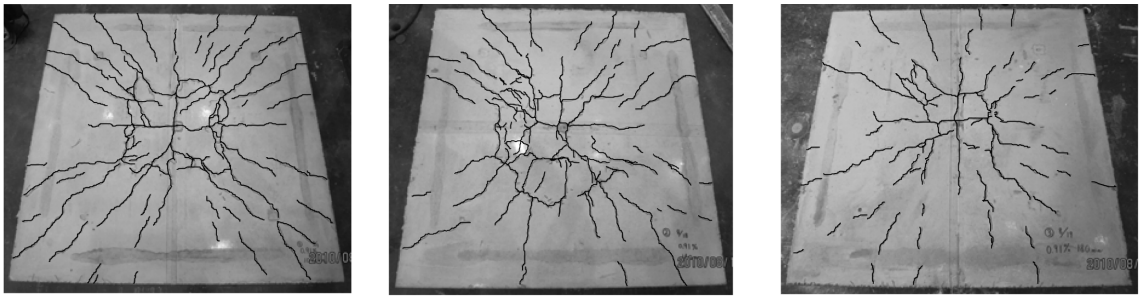

(a) Slab thickness 100 mm
(b) Slab thickness 140 mm
(c) Slab thickness 180 mm

Fig. 5 Typical cracking patterns on the bottom surface of slabs with V_f = 0.91%.

punching shear capacity of SFRC slabs became insensible from the fiber volume fraction of around 0.7%.

4.2 Cracks

Typical cracking patterns on the bottom surface of SFRC slabs with the fiber volume fraction of 0.91% after the testing are presented in Fig. 5. Grid type of cracks occurred under the loading area due to the bending moment and tangential cracks spread from the loading area to the slab corners due to the torsional moment. By increasing the slab thickness, it was noted that the crack formation in a tangential direction decreased. On the top surface, the loading pad began to sink when the punching shear cracks became wider. All SFRC slabs failed in punching shear.

From the test results conducted by Narayanan and Darwish,[3] the observed distance from the center of the slab to the intersection of the diagonal shear crack and the plane of tension steel reinforcement decreased, as the fiber factor became greater. Therefore, two SFRC slabs of 180 mm thick with the fiber volume fraction of 0.72% and 0.91% were sawn by a concrete cutter along the center line to observe the distance from the center of the slab to the diagonal shear crack. The cross sections of the SFRC slabs after cutting are shown in Fig. 6. The angles of the diagonal shear cracks were about 45 degrees in the compressive zone of the slabs and gradually decreased toward the plane of tension reinforcement. These diagonal shear cracking patterns were typically observed in both normal-weight concrete and lightweight concrete slabs.[18,19]

The measured distance from the center of the slab to the diagonal shear crack of SFRC slab with the fiber volume fraction of 0.91% decreased to 86% of the distance specified in the JSCE standard specifications.[15] On the other hand, the reduction of the measured distance in SFRC slab with the fiber volume fraction of 0.72% was not seen in comparison with the distance specified in the JSCE standard specifications.[15] It could not be revealed in this study due to the limitation of the observed data. The direction of tensile crack is affected by the boundary condition and stress distribution.[20] For plain concrete, all tensile forces are carried by the steel reinforcement at the place of the crack. In contrast, for SFRC, the concrete after tensile cracking partially resists the tensile forces by the contribution of fiber bridging. The fiber pull-out forces are transferred across the crack surfaces. The direction of principal stress combined with normal and shear stresses varies depending on those stress values. Although it is simple consideration, the angle of the principal stress decreases with increasing the fiber pull-out stress which becomes grater with the fiber volume fraction. Further studies are still needed to confirm this phenomenon.

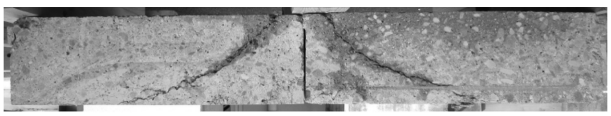

(a) Test slab of t180-0.72

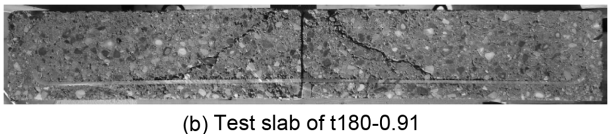

(b) Test slab of t180-0.91

Fig. 6 Diagonal shear cracks in slabs.

4.3 Proposed design equation

In this study, the design equation is considered based on the JSCE equation[15] for the punching shear capacity of reinforced concrete slabs shown above. Namely, the fiber pull-out strength presented by Narayanan and Kareem-Palanjian[13] and the perimeter of the critical section empirically modified by the fiber factor as Narayanan and Darwish[3] proposed were taken into account as follows:

$$V_u = \beta_d \beta_p \beta_r (f_{pcd} + v_b) u_p d \tag{16}$$

$$f_{pcd} = 0.2\sqrt{f_c'} \tag{17}$$

$$v_b = 0.41\,\tau F \tag{18}$$

$$\beta_d = \sqrt[4]{\frac{1000}{d}} \tag{19}$$

$$\beta_p = \sqrt[3]{100\rho} \tag{20}$$

$$\beta_r = 1 + \frac{1}{1 + 0.25u/d} \tag{21}$$

$$u_p = (u + \pi d)(1 - KF) \tag{22}$$

$$F = \frac{L}{D} V_f d_f \tag{23}$$

where f'_c is the cylindrical compressive strength of SFRC (N/mm^2), d is the average effective depth (mm), ρ is the average tension steel reinforcement ratio, τ is the average fiber-matrix interfacial bond stress taken as 4.15 N/mm^2, u is the perimeter of the loading pad (mm), and u_p is the perimeter of the critical section located at a distance of d/2 from the edge of the loading pad (mm), V_f is the fiber volume fraction, d_f is the bond factor, L and D are the length and the diameter of fiber (mm), respectively, F is the fiber factor, and K is the non-dimensional constant value (= 0.32). The values of f_{pcd}, β_d, and β_p are limited to 1.2 N/mm^2, 1.5, and 1.5.

From the results of 12 SFRC slabs conducted in this study, the constant value, K was derived as 0.32. Consequently, the mean value of the ratios (the test values conducted in this study to the predicted values) was 0.999 with a standard deviation of 0.144.

4.4 Comparisons of design equations

The proposed design equation was further applied to 50 SFRC slabs referred in the literature[1-3,6,9,12] as given in Table 4 in order to verify the accuracy. These data cover compressive strength (22 N/mm^2 to 61 N/mm^2), slab thickness (60 mm to 180 mm), tension reinforcement ratio (0.4% to 2.7%), and fiber volume fraction (0.25% to 1.93%) as well as the fiber type (hooked-ends, crimped, twisted, corrugated, and indented). In this study, if the compressive strength was determined from the cubic specimens in the literature, the cylindrical compressive strength was assumed to be equal to 0.8 times of the cubic compressive strength in the prediction.

As shown in Fig. 7, the ratios (the test values to the predicted values by the proposed equation, but neglecting the constant value: $K = 0$) for totally 62 SFRC slabs including the test results in this study significantly relate to the fiber factors. The ratios

Table 4 Details of test data and predicted values.

References	Thickness (mm)	Effective depth (mm)	Reinforce-ment ratio (%)	Fiber volume fraction (%)	Length of loading pad (mm)	Compressive strength (N/mm^2)	Maximum load (kN)	Predicted value (kN)
This study	100	70	0.85	0.67	100	24.6	137.5	121.5
	140	110	0.54	0.67	100	24.6	210.2	212.7
	180	150	0.40	0.67	100	24.6	297.6	321.0
	100	65	0.91	0.72	100	42.4	140.8	127.9
	140	105	0.57	0.72	100	42.4	213.2	230.9
	180	145	0.41	0.72	100	42.4	290.7	353.4
	100	65	0.91	0.91	100	21.6	120.8	116.1
	140	105	0.57	0.91	100	21.6	183.1	209.5
	180	145	0.41	0.91	100	21.6	231.2	320.6
	100	70	0.85	0.63	100	27.8	152.3	124.5
	100	70	0.85	0.94	100	31.1	147.9	142.2
	100	70	0.85	1.03	100	30.4	158.9	144.6
Swamy and Ali[1]	125	100	0.56	0.6	150	41.4	243.6	300.9
	125	100	0.56	0.9	150	40.1	262.9	325.0
	125	100	0.56	1.2	150	39.2	281.0	328.1
	125	100	0.56	0.9	150	40.4	267.2	325.0
	125	100	0.56	0.9	150	44.0	255.7	325.0
	125	100	0.56	0.9	150	39.4	262.0	325.0
	125	100	0.56	0.9	150	39.1	249.0	323.1
	125	100	0.56	0.9	150	41.7	236.7	315.6
Hirasawa, et al.[2]	100	75	0.95	1.0	120	51.2	226.5	199.6
	100	75	0.86	1.0	120	51.2	204.0	193.1
	100	75	0.76	1.0	120	51.2	212.8	185.3
	100	75	0.67	1.0	120	51.2	178.5	177.7
	100	75	0.95	1.5	120	60.8	249.1	218.5
	100	75	0.86	1.5	120	60.8	203.0	211.4
	100	75	0.76	1.5	120	60.8	222.6	202.8
	100	75	0.67	1.5	120	60.8	204.0	194.5
	100	75	0.95	2.0	120	50.3	263.8	227.4
	100	75	0.86	2.0	120	50.3	223.6	219.9
	100	75	0.76	2.0	120	50.3	203.0	211.1
	100	75	0.67	2.0	120	50.3	205.0	202.4
Narayanan and Darwish[3]	60	45	2.01	0.25	100	55.3	93.4	86.8
	60	45	2.01	0.5	100	47.5	102.0	98.3
	60	45	2.01	0.75	100	48.9	107.5	108.2
	60	45	2.01	1.0	100	56.3	113.6	115.9
	60	45	2.01	1.25	100	56.4	122.2	121.4
	60	45	2.01	1.0	100	49.9	92.6	115.9
	60	45	2.24	1.0	100	48.1	111.1	120.2
	60	45	2.46	1.0	100	46.2	111.3	124.0
	60	45	2.69	1.0	100	50.6	113.3	127.8
	60	45	2.01	1.0	100	31.6	82.1	112.4
	60	45	2.01	1.0	100	34.4	84.9	114.7
Shaarban and Gesund[6]	82.55	60	1.56	0.61	63.5	34.5	94.5	89.1
	82.55	60	1.56	0.61	63.5	37.3	112.5	90.8
	82.55	60	1.56	0.61	63.5	29.7	72.0	83.5
	82.55	60	1.56	0.92	63.5	37.7	108.0	94.9
	82.55	60	1.56	1.22	63.5	46.8	135.0	98.7
	82.55	60	1.56	1.22	63.5	36.6	117.0	98.7
	82.55	60	1.56	1.84	63.5	22.4	99.0	90.1
	82.55	60	1.56	1.93	63.5	22.1	103.5	90.8
Wakabayashi and Maruyama[9]	70	58	1.37	0.5	60	48.5	94.1	91.5
	70	58	1.37	1.0	60	49.2	111.5	106.1
	70	58	1.37	1.5	60	49.0	114.6	116.8
Cheng and Parra-Montesinos[12]	152	127	0.83	1.0	152	25.4	386	419.2
	152	127	0.56	1.0	152	25.4	389	367.7
	152	127	0.83	1.5	152	59.3	530	520.3
	152	127	0.56	1.5	152	57.9	444	456.4
	152	127	0.83	1.5	152	31.0	522	485.2
	152	127	0.56	1.5	152	31.0	472	425.7
	152	127	0.83	1.5	152	46.1	530	523.8
	152	127	0.56	1.5	152	59.1	503	459.5

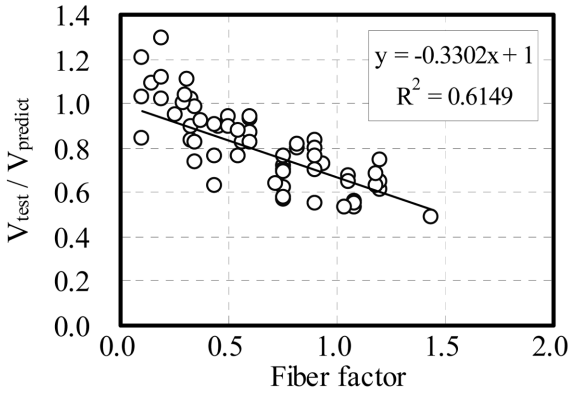

Fig. 7 Relationship between punching shear capacity ratio and fiber factor.

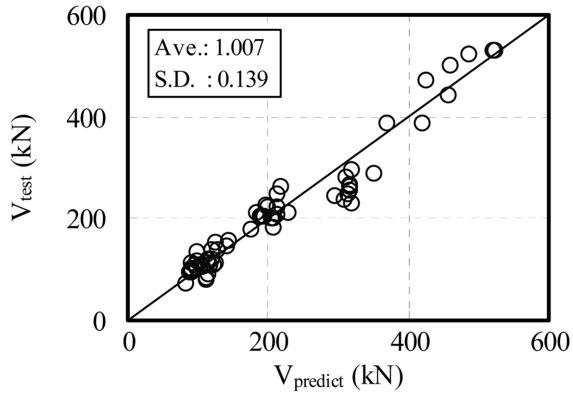

Fig. 8 Relationship between test value and predicted value.

decrease linearly with increasing fiber factors. A straight line was fitted to those data in Fig. 7 to obtain the slope value. Then, the slope value of 0.33 considerably agrees well with the value of 0.32 derived from the test results conducted in this study.

From the results of comparisons for 62 SFRC slabs as shown in Table 4 and Figure 8, the mean value of the ratios (the test values to the predicted values) was 1.007 with a standard deviation of 0.139. The proposed design equation can predict the punching shear capacity of SFRC slabs with an applicable accuracy.

Furthermore, the predicted results were compared with the design equation presented by Narayanan and Darwish[3] shown above. In the design equation presented by Theodorakopoulos and Swamy,[11] the yield strength of tension steel reinforcement is needed to calculate a parameter. The yield strength data were limited to be available in some referred literatures. Then, it would be avoided to compare with their proposed design equation. Consequently, it is noticed that the proposed design equation has almost the same predicting accuracy in comparison with the design equation presented by Narayanan and Darwish[3], in which the mean value of the ratios (the test values to the predicted values) was 0.980 with a standard deviation of 0.198.

5. Conclusions

This study investigated the design equation for the punching shear capacity of SFRC slabs based on the JSCE equation taking into account the fiber pull-out strength and the perimeter of the critical section depending on the fiber factor. Punching shear tests for 12 SFRC slabs were carried out in this study in order to derive the constant value, K. As a result, the constant value, K was determined to be 0.32. Furthermore, to verify the accuracy of the proposed design equation, the punching shear capacities of 50 SFRC slabs conducted by earlier researchers were predicted and the results were compared with the design equation proposed by Narayanan and Darwish. Then, the design equation proposed in this study predicted the punching shear capacity of SFRC slabs with an applicable accuracy.

References

1. Swamy, R. N. and Ali, S. A. R., "Punching Shear Behavior of Reinforced Slab-Column Connections Made with Steel Fiber Concrete," *ACI Journal*, Vol. 79, 1982, pp. 392~406.

2. Hirasawa, M, Ito, K., and Takagi, K., "Punching Shear Strength of Steel Fiber Reinforced Concrete Slabs," *Proceedings of the 37th Annual Conference of the JSCE*, V-124, 1982, pp. 247~248.

3. Narayanan, R. and Darwish, I. Y. S, "Punching Shear Tests on Steel-Fibre-Reinforced Micro-Concrete Slabs," *Magazine of Concrete Research*, Vol. 39, No. 138, 1987, pp. 42~50.

4. Alexander, S. D. B. and Simmonds, S. H., "Punching Shear Tests of Concrete Slab-Column Joints Containing Fiber Reinforcement," *ACI Structural Journal*, Vol. 89, No. 4, 1992, pp. 425~432.

5. Tan, K. H. and Paramasivam, P., "Punching Shear Strength of Steel Fiber Reinforced Concrete Slabs," *Journal of Materials in Civil Engineering*, Vol. 6, No. 2, 1994, pp. 240~253.

6. Shaaban, A. M. and Gesund, H., "Punching Shear Strength of Steel Fiber Reinforced Concrete Flat Plates," *ACI Structural Journal*, Vol. 91, No. 3, 1994, pp. 406~414.

7. Di Prisco, M. and Felicetti, R., "Some Results on Punching Shear in Plain and Fibre-Reinforced Micro-Concrete Slabs," *Magazine of Concrete Research*, Vol. 49, No. 180, 1997, pp. 201~219.

8. McHarg, P. J., Cook, W. D., Mitchell, D., and Yoon, Y. S., "Benefits of Concentrated Slab Reinforcement and Steel Fibers on Performance of Slab-Column Connections," *ACI Structural Journal*, Vol. 97, No.2, 2000, pp. 225~234.

9. Wakabayashi, M. and Maruyama, T., "A Study on Punching Shear Resistance of Reinforced Concrete Slab by Using Steel Fiber," *Proceedings of the 57th Annual Conference of the JSCE*, V-131, 2002, pp. 261~262.

10. Theodorakopoulos, D. D. and Swamy, R. N., "Ultimate Punching Shear Strength Analysis of Slab-Column Connections with Steel Fibers," ACI SP-182-11, 1999, pp. 181~214.

11. Theodorakopoulos, D. D. and Swamy, R. N., "A Design Method for Punching Shear Strength of Steel Fiber Reinforced Concrete Slabs," *Innovations in Fiber-Reinforced Concrete for Value*, ACI SP-216, 2003, pp. 181~202.

12. Cheng, M. Y. and Parra-Montesinos, G. J., "Evaluation of Steel Fiber Reinforcement for Punching Shear Resistance in Slab-Column Connections Part I: Monotonically Increased Load," *ACI Structural Journal*, Vol. 107, No. 1, 2010, pp. 101~109.

13. Narayanan, R. and Kareem-Palanjian, A. S., "Effect of Fibre Addition on Concrete Strengths," *Indian Concrete Journal*, Vol. 58, No. 4, 1984, pp. 100~103.

14. Narayanan, R. and Darwish, I. Y. S, "Use of Steel Fibers as Shear Reinforcement," *ACI Structural Journal*, Vol. 84, No. 3, 1987, pp. 216~227.

15. JSCE, "Standard Specifications for Concrete Structures-2007, Design," 2008.

16. JSCE, "Standard Specifications for Concrete Structures - 2005, Test Methods and Specifications," 2005.

17. Mindess, S., Adebar, P., and Henley, J., "Testing of Fiber-Reinforced Structural Concrete Elements," *Proceedings of ACI International Conference on High-Performance Concrete: Design and Materials and Recent Advances in Concrete Technology*, ACI SP-172, 1997, pp. 495~515.

18. Higashiyama, H., Matsui, S., and Uchida, Y., "Punching Shear Capacity of RC Slabs with Lightweight Concrete," *Proceedings of 2nd International Conference on Bridge Maintenance, Safety, Management and Cost*, Kyoto, Japan, 2004, S14-07.

19. Kariya, T., Takemura, H., Nishihara, S., Fukunaga, A., Furuichi, T., Fukuda, H., Higashiyama, H., and Matsui, S., "Punching Shear Capacity of RC Slabs and Deterioration Survey for PC T-beams in the Omori Overpass Bridge," *Proceedings. of the 6th Korea-Japan Joint Seminar on Bridge Maintenance*, Yongpyong Resort, Korea, 2007, pp. 175~186.

20. Choi, K. K., Park, H. G, and Wight, J. K., "Shear Strength of Steel Fiber-Reinforced Concrete Beams without Web Reinforcement," *ACI Structural Journal*, Vol. 104, No. 1, 2007, pp. 12~21.